



Inhibition of inducible nitric oxide synthase by bis(helenaliny)glutarate in RAW264.7 macrophages

V. Badireenath Konkimalla^a, Martina Blunder^b, Rudolf Bauer^b, Thomas Efferth^{a,*}

^a German Cancer Research Centre, Pharmaceutical Biology (C015), Heidelberg, Germany

^b Institute of Pharmaceutical Sciences, Karl-Franzens-University Graz, Austria

ARTICLE INFO

Article history:

Received 4 November 2009

Accepted 18 January 2010

Keywords:

Cytotoxicity
Glucocorticoid receptor signaling pathway
Griess assay
Interleukin-10 signaling pathway
Microarrays
Nitric oxide

ABSTRACT

Nitric oxide (NO) plays a role in various physiological and pathophysiological conditions such as immunoregulatory and inflammatory processes. Hence, NO and its generating enzyme, inducible nitric oxide synthase (iNOS) may not only be of diagnostic and prognostic value, but may also serve as targets for novel therapeutic options. In the present investigation, we have screened a phytochemical library by correlating the IC₅₀ values for 531 natural products of 60 cell lines with the microarray-based mRNA expression of 95 genes known to be involved in NO metabolism and signaling with the aim to identify candidate compounds as inhibitors for NO metabolism and signaling. We identified bis(helenaliny)glutarate (BHG) as putative candidate compound. Indeed, BHG inhibited NO production (IC₅₀ value: 0.90 ± 0.04 μM) and down-regulated iNOS protein expression (IC₅₀ value: 1.12 ± 0.16 μM) of RAW264.7 mouse macrophages in the presence of lipopolysaccharide. Performing XTT cytotoxicity assays, we found that BHG inhibited cell growth in a dose-dependent manner with an IC₅₀ value of 5.6 μM. To gain insight into molecular pathways involved in NO inhibition and cytotoxicity, we performed microarray experiments which were exemplarily validated by real-time RT-PCR. A total of 227 genes (67 up- and 160 down-regulated) were obtained, which exhibited significant differences in mRNA regulation between BHG-treated and untreated RAW264.7 macrophages. Sixteen of 227 genes are known to be involved in NO-signaling. Pathway analyses revealed that further five and four down-regulated genes belong to the glucocorticoid receptor and interleukin-1 and interleukin-10 pathways, respectively. An interference of these two pathways and NO is known for inflammation and auto-immune diseases. The therapeutic potential of this compound has to be explored in the future.

© 2010 Elsevier Inc. All rights reserved.

1. Introduction

Nitric oxide (NO) is a gaseous free radical produced by inducible nitric oxide synthase (iNOS) and other enzymes from the amino acid L-arginine. It plays a role in various physiological and pathophysiological conditions such as immunoregulatory and inflammatory processes. NO is involved in cancer, rheumatoid arthritis, diabetes, liver cirrhosis, septic shock, cardiovascular diseases, etc. [1,2]. Sustained induction of iNOS, may be mutagenic, through NO-mediated DNA damage or hindrance to DNA repair, and thus potentially carcinogenic [3–6]. NO can stimulate tumor growth and metastasis by promoting migratory, invasive, and angiogenic abilities of tumor cells [7–10]. Higher amounts of NO and iNOS were found in tumors compared to normal tissues [11–15], and iNOS expression in tumors was an unfavorable prognostic

factor for survival times of cancer patients [16–19]. NO and iNOS may not only be of diagnostic and prognostic value, but may also serve as targets for novel therapeutic options [20–22].

There is a large body of evidence that phytochemicals inhibit NO production [8,23]. During the past few years, molecular modes of action elicited by phytochemicals have been described, including the inhibition of iNOS or COX-2 expression [24] and inhibition of NO or prostaglandin E-2 production [25–27]. Phytochemical NO inhibitors suppress the production of specific cytokines such as TNF-α, IL-1, IL-6, or IL-10 [28–31]. The transcription factor NFκB seems to play a pivotal role during mediation of these effects. Several phytochemicals with NO inhibitory activity have been shown to suppress activation and translocation of NFκB from the cytoplasm to the nucleus [31–34]. Furthermore, some phytochemicals inhibiting NO production and NFκB activation also suppressed the activation of mitogen-activated protein (MAP) kinases such as the stress-activated protein kinase (SAPK)/c-JUN N-terminal kinase (JNK) [34].

NO inhibition by phytochemicals may therapeutically be exploited for immunomodulation and anti-inflammatory responses [35], treatment of Leishmania infections [36], anti-adrenergic

* Corresponding author at: Department of Pharmaceutical Biology, Institute of Pharmacy and Biochemistry, University of Mainz, Staudinger Weg 5, 55128 Mainz, Germany. Tel.: +49 6131 39 25751; fax: +49 6131 3923752.

E-mail address: efferth@uni-mainz.de (T. Efferth).

responses [37], lowering blood pressure [38], spasmolysis [39], etc. Hence, phytochemicals represent a valuable source to develop drugs for the prevention and treatment of diseases, where NO plays a role.

Previously, we established a library of more than 2400 phytochemicals, 531 of which were cytotoxic towards cancer cells [40]. In the present investigation, we have screened this library and identified bis(helenalinyl)glutarate (BHG) as putative candidate compound, because of the significant relationship of the IC₅₀ values for BHG of 60 cell lines and the microarray-based mRNA expression values of these cell lines.

BHG is a natural product derived from *Helenium microcephalum* [41]. Then, we analyzed BHG for its potential to inhibit NO generation and iNOS protein expression in RAW264.7 mouse macrophage cells. RAW264.7 cells represent a well-established experimental system for studying nitric oxide biology. XTT assays were performed to determine the cytotoxic activity of the compound. To gain insight into molecular players involved in nitric oxide inhibition and cytotoxicity, we performed microarray experiments which were exemplarily validated by real-time RT-PCR.

2. Material and methods

2.1. Compound

Bis(helenalinyl)glutarate (BHG) was obtained from the Drug Synthesis and Chemistry Branch of the National Cancer Institute (Bethesda, Maryland, USA). The chemical structure is depicted in Fig. 1.

2.2. Cells

RAW264.7, a mouse macrophage cell line was in Dulbecco's Modified Eagle Medium (DMEM, PAA Laboratories, Cölbe, Germany) supplemented with 2 mM glutamine, antibiotics (100 U/mL penicillin A and 100 U/mL streptomycin), and 10% heat-inactivated foetal bovine serum (FBS; PAA Laboratories) and maintained in a 37 °C humidified incubator containing 5% CO₂. Twenty-four hours before starting the experiments cells were seeded in 24-well or 6-well tissue culture plates in a density of 10⁶ or 2 × 10⁶ cells/mL for measurement of NO release or iNOS expression, respectively.

2.3. Measurement of NO release (by Griess assay)

Lipopolysaccharide (LPS, Sigma–Aldrich, Munich, Germany) and γ -interferon (IFN- γ ; Roche) have a synergistic effect on iNOS expression. LPS and IFN- γ activate iNOS expression pathway [42,43].

iNOS causes the release of NO by converting L-arginine to L-citrulline. Therefore, RAW264.7 cells were stimulated with 0.5 μ g/

mL LPS and 50 U/mL IFN- γ in presence or absence of BHG. Nitrite release was measured as previously described [44]. Each experiment was performed at least four times in duplicate and was compared with a standard curve plotted against different concentrations of sodium nitrite [45] with slight modifications [44]. IC₅₀ determinations were performed in ten concentrations (0.001, 0.003, 0.01, 0.03, 0.1, 0.3, 1, 3, 10, 30 μ M) in at least eight independent experiments, each time in duplicate, and the IC₅₀ values were calculated with the SigmaPlot program package employing the 4-parameter logistic regression model.

2.4. Western blot analysis

iNOS gene expression was induced by treating RAW264.7 macrophages with LPS and IFN- γ as described above. SDS–polyacrylamide gel electrophoresis and Western blotting were performed similarly to previous reported methods [46]. In brief, cells were harvested, washed twice with PBS, centrifuged, re-suspended and homogenized by three-fold sonication. Protein concentrations were assessed using the Bradford Assay (Sigma–Aldrich) to allow loading of equal protein amounts per lane onto 8% SDS–polyacrylamide gels. The proteins were separated by electrophoresis and then transferred to nitrocellulose membranes by electroblotting. iNOS was detected with an anti-iNOS antibody, using horseradish peroxidase-conjugated anti-mouse IgG. After developing the immunoblots by the ECL system (Amersham Pharmacia Biotech) they were analyzed using a Herolab E.A.S.Y. Win32 HiRes densitometric system additionally equipped with an UV Transilluminator (UVT-28 ME). Western blot analysis was conducted with cells treated with different concentrations of BHG (0.1, 0.3, 1, 3, 10 μ M) obtained from four independent experiments.

2.5. XTT proliferation assay

Inhibition of proliferation was assessed using the standard 2,3-bis[2-methoxy-4-nitro-5-sulphophenyl]-2H-tetrazolium-5-carboxanilide inner salt (XTT) assay kit (Roche, Indianapolis, IN), which measures the metabolic activity of viable cells [47]. The toxicity of compounds was determined by means of the Cell Proliferation Kit II (Roche Diagnostics, Mannheim, Germany) as previously described by us [44]. This test is based on the cleavage of the yellow 2,3-bis[2-methoxy-4-nitro-5-sulphophenyl]-2H-tetrazolium-5-carboxanilide inner salt (XTT) by ubiquitous dehydrogenases leading to the formation of an orange formazan dye. The amount of dye is commensurate to the number of metabolic active cells. IC₅₀ determinations of BHG were performed in ten concentrations (0.001, 0.003, 0.01, 0.03, 0.1, 0.3, 1, 3, 10, 30 μ M). Corresponding DMSO concentrations served as negative control.

2.6. RNA isolation

Total RNA of RAW264.7 cells was extracted from the test samples using RNeasy[®] mini kit (Qiagen Inc., Valencia, CA, USA) according to the manufacturer's instructions to obtain highly pure RNA. The concentration and quality of total RNA was verified by electrophoresis using the total RNA Nano chip assay on an Agilent 2100 Bioanalyzer (Agilent Technologies GmbH, Berlin, Germany). Only samples with RNA index values greater than 8.5 were selected for expression profiling. RNA concentrations were determined using the NanoDrop spectrophotometer (NanoDrop Technologies, Wilmington, DE).

2.7. Probe labelling and Illumina Sentrix BeadChip array hybridization

Biotin-labelled cRNA samples for hybridization on Illumina Mouse Sentrix-8 BeadChip arrays (Illumina Inc., San Diego, CA,

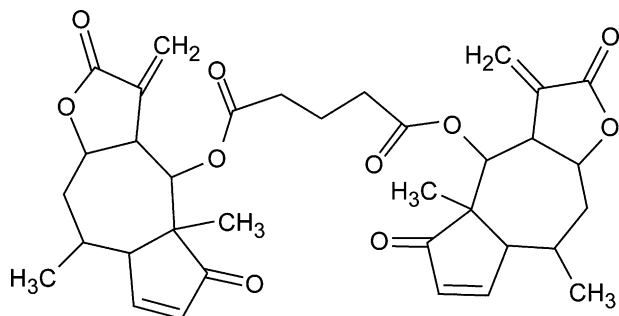


Fig. 1. Chemical structure of bis(helenalinyl)glutarate.

Table 1

Primer sequences of genes analyzed by real-time RT-PCR.

Gene	EST	Forward primer 5' to 3'	Reverse primer 5' to 3'
<i>Atf4</i>	NM_009716.2	atgatggcttgccagtg	ccatttttccaacatccaatc
<i>Bcl2</i>	NM_009741.3	gtacctgaaccggcatctg	ggggccatatagttccacaa
<i>Ccl2</i>	NM_011333.3	ggctggagagctacaagagg	ctcttgagcttggtgacaaaa
<i>Ccne1</i>	NM_007633.2	acagcttgatttgctgga	gggggtgtcaggaccacact
<i>Cd40</i>	NM_170701.2	ggaacgagtcagactaatgtcatc	tctcctgagcactcactgatataga
<i>Csf3</i>	NM_009971.1	gctgctggagcagttgtg	gggatccccagagagtg
<i>Icam1</i>	NM_010493.2	gctaccatcacctgtattcg	aggtccttgctactgtctg
<i>IL-1b</i>	NM_008361.3	caggcaggcagtatcactca	gtcacagaggatgggctctt
<i>Irf1</i>	NM_008390.1	cctgggtcaggacttgata	gagactgtgctgacgacac
<i>Itgal</i>	NM_008400.2	cctctgtcttctgttcctg	ctccttcagggtccgttga
<i>Mapkapk2</i>	NM_008551.1	cagcaaaaattcgccctaaa	agtgcagctccacctctctg
<i>Myd116</i>	NM_008654.1	acgatcgctttggcaac	gacatgctgggtcttgg
<i>Nos2</i>	NM_010927.3	ctttgccacggacgagac	tcattgtactctgagggtgac
<i>Tnfrsf1b</i>	NM_011610.3	ggctcagatgtgtgtgcta	ccgagggtctgttgacagaa
<i>Tyk2</i>	NM_018793.2	ggccacgagtactaccagtg	gcattctggggcatacca
Reference genes			
<i>ALAS1</i>	NM_020559.2	ccctccagccaatgagaa	gtgccatctgggactcgt
β -Actin	NM_007393.3	ctaaggccaacctgaaaag	accagaggcatcagggaca
<i>HPRT</i>	NM_013556.2	ggagcggtagcacctct	ctggttcacatcgctaatac

USA) were prepared according to Illumina's recommended sample labelling procedure based on a previously published protocol [48].

Hybridization was performed as previously described [44].

2.8. Scanning and data analysis

Microarray scanning was done using a bead station array scanner, setting adjusted to a scaling factor of 1 and PMT settings at 430 [44]. Pathway analysis was done by using the Ingenuity Pathways Analysis software (version 5.5) from Ingenuity Systems (Redwood City, CA, USA).

2.9. Real-time (RT)-PCR

The experiments were done on the Roche LC480 using ABgene Mastermix "CM 215-A" and Roche Universal Probe Library as previously described [44]. Oligos were designed using Roche ProbeFinder Webservice (<https://qpcr2.probefinder.com/organism.jsp>) and were synthesized by MWG. Two versions were designed per gene. All analyzed variants span an intron to prevent cross reactions with possible genomic DNA contamination.

Genes identified by microarray analyses were exemplarily analyzed for validation by means of real-time RT-PCR. The housekeeping genes, ALAS1, β -actin, and HPRT, served as reference. The primer sequences are shown in Table 1. All measurements are done in triplicates to calculate mean values and standard deviations.

3. Results

3.1. Computational approach

As a start-up approach, we identified candidate compounds by correlating the IC_{50} values for 531 natural products of 60 cell lines from our database [24] with the microarray-based mRNA expression of 95 genes known to be involved in NO metabolism and signaling (Supplementary Table 1).

The best correlation was found between the mRNA expression of the *TXNRD1* gene coding for thioredoxin reductase 1 and the compound, bis(helenaliny)glutarate (BHG) (Pearson's correlation analysis $R > 0.6$). The role of thioredoxin reductase 1 for oxidative and nitrosative stress is well known [31–33]. Therefore, to experimentally validate the mathematical approach experimentally and to prove an iNOS inhibitory effect of BHG on NO-signaling

pathways, RAW264.7 mouse macrophages were investigated. Because the RAW264.7 cell line represents a well-known gold standard model system for studying nitric oxide biology, it was used to perform further experiments.

3.2. Measurement of NO release (by Griess assay)

After 16 h incubation, BHG inhibited NO generation in a dose-dependent manner by testing ten different concentrations (0.001, 0.003, 0.01, 0.03, 0.1, 0.3, 1, 3, 10, 30 μ M) (Fig. 2A). The IC_{50} value was $0.9 \pm 0.04 \mu$ M. DMSO (0.1%)-treated cells were used as vehicle control.

3.3. Western blot analysis

Furthermore, decreased expression of iNOS was shown by performing Western blot experiments at different concentrations (Fig. 2B). Quantitative analysis of the Western blot resulted in an IC_{50} of $1.1 \pm 0.16 \mu$ M.

3.4. XTT assay

To analyze, whether inhibition of NO generation is associated with cytotoxicity, LPS-induced RAW264.7 cells were treated with BHG at concentrations ranging from 10^{-3} to 10^{-9} M. As shown in Fig. 3, BHG inhibited viability of cells in a dose-dependent manner with an IC_{50} value of 5.6 μ M.

3.5. Quality control of microarray analysis

Several quality control tests were performed to ensure proper hybridization results as previously described [44]. We assured

- Linearity of concentration-dependent signal change (low, medium, and high concentrations) of target Cy3 hybridization target control oligonucleotides. This is necessary to yield a gradient hybridization response.
- Low signals of mismatched controls in comparison to perfect matches implied that the hybridization and washing was adequately stringent.
- Low signals of raw data background (non-related probes) and system noise implied that the imaging system background as well as any signal resulting from non-specific binding of dye or cross-hybridization were satisfactorily small.
- Similarity of biological replicates by cluster analysis.

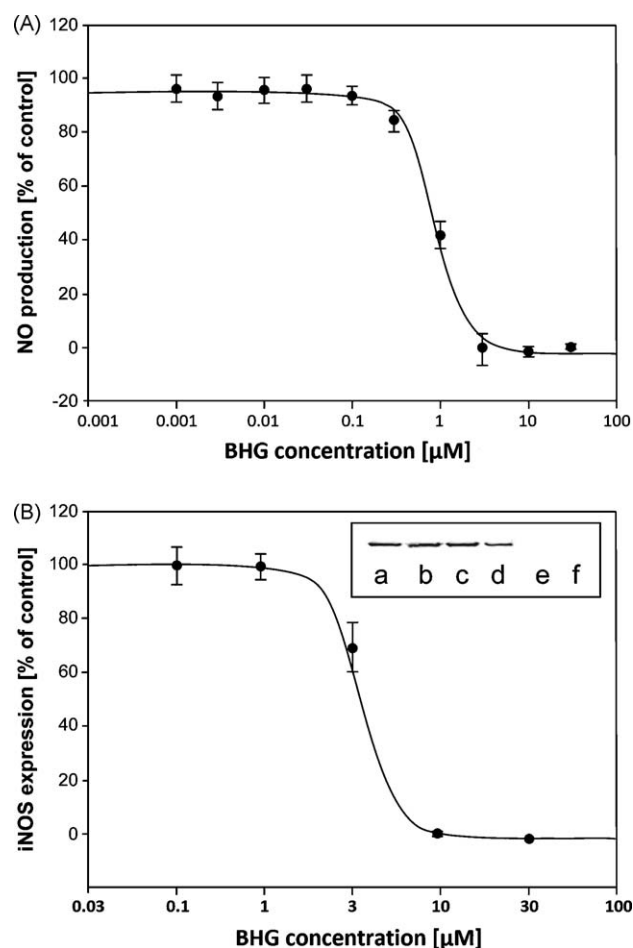


Fig. 2. Inhibition of nitric oxide (NO) production and inducible NO synthase (iNOS) expression by bis(helenalanyl)glutarate (BHG) in mouse macrophage cells (RAW264.7). (A) Graphical representation of the IC_{50} determination of the inhibitory activity on NO production of BHG as determined by the Griess assay. Ten different concentrations (ranging from 0.001 to 30 μ M) were tested. 0.1% DMSO was used as vehicle control. Data are represented as nitrite formation in % of vehicle control and are expressed as mean values \pm standard deviation of at least eight independent experiments, each time performed in duplicates. (B) Graphical representation of the IC_{50} determination of the inhibitory activity on iNOS expression of BHG as determined by Western blot analysis. Five different concentrations (ranging from 0.1 to 10 μ M) were tested. 0.1% DMSO was used as vehicle control. Data are represented as iNOS expression in % of vehicle control and are expressed as mean values \pm standard error of mean of four independent experiments. (Insert in B) Western blot analysis of the inhibitory activity on iNOS expression of BHG. Five different concentrations (ranging from 0.1 to 10 μ M) were tested. 0.1% DMSO was used as vehicle control. ((a) 0.1% DMSO, (b) BHG 0.1 μ M, (c) BHG 0.3 μ M, (d) BHG 1 μ M, (e) BHG 3 μ M, (f) BHG 10 μ M).

3.6. Microarray hybridization and pathway analysis

LPS-induced RAW264.7 cells were treated with BHG (4 μ g/mL) for 24 h. DMSO-treated cells served as controls. High quality total RNA was isolated and subjected to hybridization on Illumina bead chip. In order to filter the false positively detected intensities from 46,643 genes, the array standard deviation cut-off was set to 2.5 and bead standard deviation to 7.5. Finally, 227 genes were obtained, which exhibited significant differences in mRNA regulation between BHG-treated and untreated RAW264.7 macrophages. Sixty-seven genes thereof were up-regulated and 160 genes were down-regulated. A literature search showed that 16 of the 227 genes are known to be involved in the NO-signaling pathway, five and four down-regulated genes belonged to the glucocorticoid receptor and IL-10 pathway, respectively (Supplementary Table II).

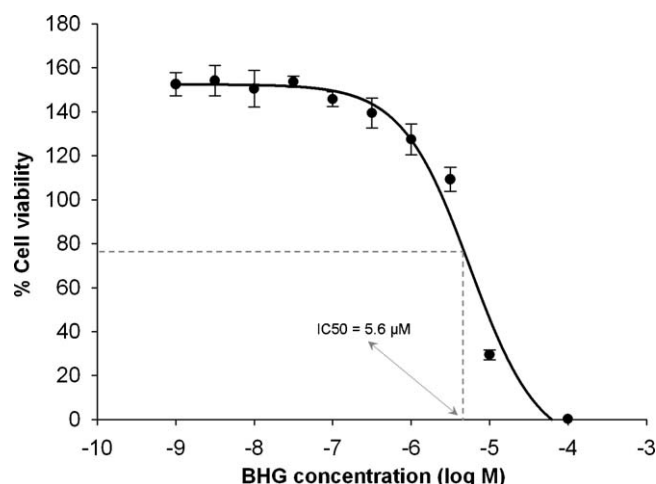


Fig. 3. Cytotoxicity of BHG towards RAW264.7 cells as determined by the XTT assay. The values of the dose response curve were normalized with the values for cells treated with 1% DMSO serving a vehicle control. Mean values of two independent experiments with each two replicates are shown.

To investigate, whether BHG elicited its activity through one or several pathways, we analyzed all 227 differentially expressed genes by means of the Ingenuity Pathway Analysis software. The top 10 out of >80 canonical significantly regulated pathways upon BHG treatment ($P < 0.05$) are shown in Fig. 4. The most prominent pathways were the glucocorticoid receptor signaling pathway (Fig. 5) and the interleukin-1 and interleukin-10 (IL-1 and IL-10) signaling pathways (Fig. 6). After treatment with BHG, we observed an up-regulation of I κ B, the inhibitor of nuclear factor- κ B (NF κ B), and a down-regulation of another protein in the NF κ B protein complex, PKAc. Furthermore, several NF κ B downstream regulated genes were down-regulated upon BHG challenge, *IL-1B*, *CCL2*, *CCL13*, *iNOS*, *Bcl-2*, and *ICAM-1* (Fig. 5). As shown in Fig. 6, IL-1 was down-regulated by BHG. Since NF- κ B is also involved in IL-1 signaling, the up-regulated I κ B expression in glucocorticoid receptor signaling (Fig. 5) was also relevant for IL-1 signaling (Fig. 6). Furthermore, *IKK* expression was down-regulated in the IL-1 signaling route. On the other hand, IL-10 signaling was affected by BHG treatment. We observed down-regulated expression levels of IL-10 receptor- α and *TYK2*. The expression of two other genes, *FCGR1* and *HMOX1* downstream of the IL-10 signaling route was also down-regulated. *HMOX1* interferes with IL-1 signaling, pointing to an interconnection of IL-1 and IL-10 signaling pathways.

3.7. Real-time RT-PCR

For exemplary validation of the mRNA expressions obtained by microarray analyses, we performed real-time RT-PCR. Fifteen genes out of 227 were known from literature to have a direct or indirect involvement in the NO-signaling pathway apart from their canonical pathways. These 15 genes were selected and were quantified by RT-PCR (Table 2). The correlation coefficient between mRNA expression values determined by microarray hybridization and real-time RT-PCR was $R^2 = 0.88$, indicating a high degree of concordance between results obtained by microarray hybridization and real-time RT-PCR.

4. Discussion

By screening a natural product database [40], we identified bis(helenalanyl)glutarate (BHG) as a potential novel inhibitor of nitric oxide production and modulator of nitric oxide-related

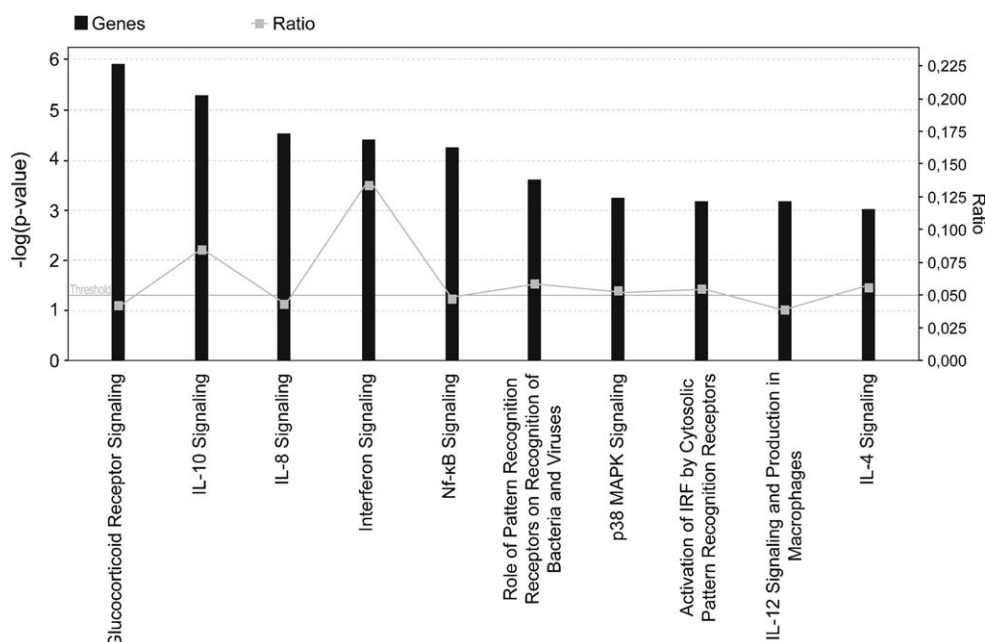


Fig. 4. Identification of canonical signaling pathways regulated upon BHG treatment in RAW264.7 cells. Gene expression of cells treated with the IC₅₀ concentration of BHG (5.6 μM) was compared to gene expression in untreated cells. The evaluation of differentially expressed genes was performed using the Ingenuity Pathway Analysis software, version 5.5 (see Section 2).

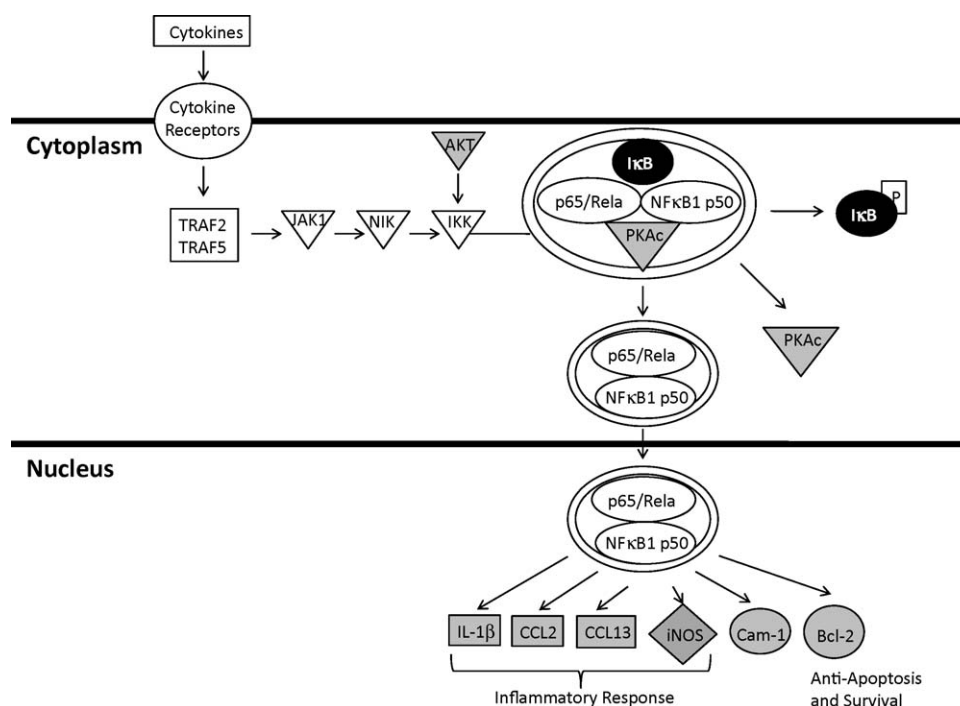


Fig. 5. Canonical glucocorticoid receptor signaling pathway regulated in RAW264.7 cells upon treatment with BHG. Pathway analysis was performed using Ingenuity Pathway Analysis tool. Eleven genes from the glucocorticoid receptor signaling pathway were regulated upon treatment with the IC₅₀ concentration of BHG (5.6 μM). The shown network was significantly associated wherein genes highlighted in *black* color indicate up-regulation while *grey* color indicate down-regulation of transcription.

signaling pathways. Cell-based approaches such as cell viability assay and nitric oxide production inhibition assay further validated that BHG is cytotoxic at micromolar range and specifically inhibited iNOS expression. The inhibition of NO production and iNOS protein expression by BHG corresponds to the down-regulation of iNOS mRNA in our microarray analyses. Hence, the inhibitory effect of BHG on NO production and iNOS expression was confirmed by several independent methods. Our genomic approach through genome-wide microarray analysis showed 227 other molecular

players that are regulated by BHG. Fifteen differentially regulated genes were selected for validation of microarray hybridization results by real-time RT-PCR. Finally, pathway analysis on all genes differentially regulated by BHG further suggests that this compound apart from exhibiting cytotoxic activity through inhibiting the expression of iNOS and affecting the NO-signaling pathway might also play a potential role in pathways related to inflammation and auto-immune disorders, e.g. the glucocorticoid receptor signaling pathway and the IL-10 signaling pathway.

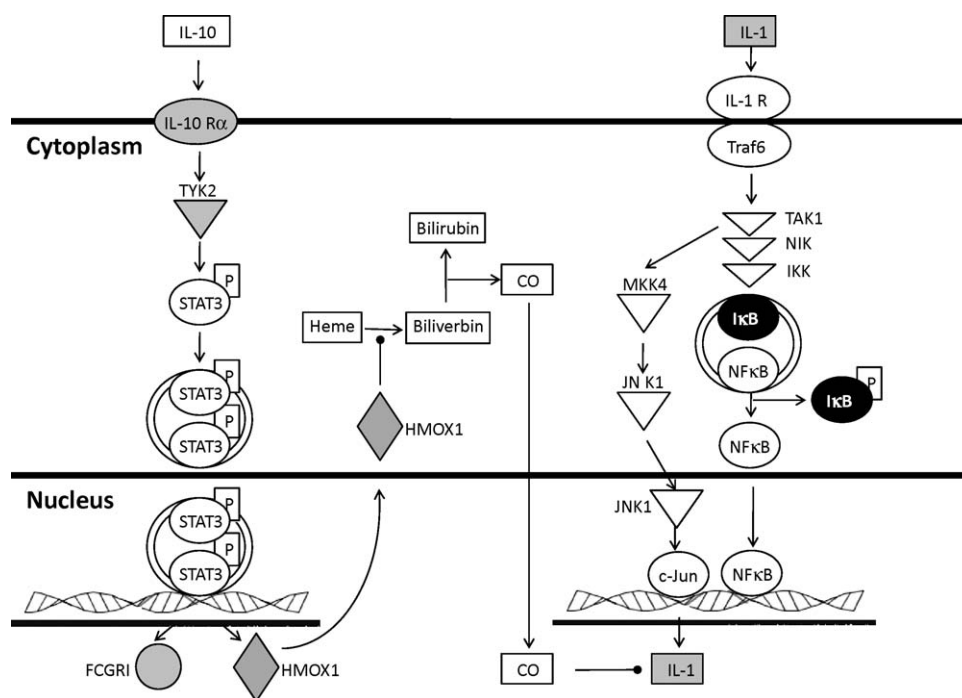


Fig. 6. Canonical IL-1 and IL-10 signaling pathways regulated in RAW264.7 cells upon treatment with BHG. Pathway analysis was performed using Ingenuity Pathway Analysis tool. Four genes from the IL-1 and five genes from the IL-10 signaling pathway were regulated upon treatment with the IC₅₀ concentration of BHG (5.6 μM). One regulated gene, *HMOX1*, belongs to both pathways. The shown network was significantly associated wherein genes highlighted in *black* color indicate up-regulation while *grey* color indicates down-regulation of transcription.

Table 2

Validation of microarray-based mRNA expression by quantitative real-time RT-PCR. Fifteen genes found to be differentially regulated in untreated and BHG-treated RAW264.7 cells were analyzed.

Gene symbol	Gene name (<i>Mus musculus</i>)	Microarray hybridization			Real-time RT-PCR		
		Untreated cells	BHG-treated cells	Fold change	Untreated cells	BHG-treated cells	Fold change
<i>Atf4</i>	Activating transcription factor 4	456.13 ± 43.63	2118.13 ± 106.74	4.64	31.3	73.133 ± 5.2080	0.43
<i>Bcl2</i>	B-cell leukaemia/lymphoma 2, transcript variant 1	280.76 ± 22.17	102.61 ± 4.35	−2.74	16.5	6.593 ± 2.3026	−2.50
<i>Ccl2</i>	Chemokine (C-C motif) ligand 2	1376.88 ± 99.17	306.22 ± 11.15	−4.5	8.24	0.402 ± 0.0907	−20.48
<i>Ccne1</i>	Cyclin E1	401.95 ± 19.70	176.66 ± 5.38	−2.28	0.728	0.189 ± 0.0689	−3.85
<i>CD40</i>	CD40 antigen, transcript variant 3	3987.22 ± 225.28	1099.48 ± 33.17	−3.63	0.00247	0.001 ± 0.0002	−2.39
<i>Csf3</i>	Colony stimulating factor 3 (granulocyte)	6927.27 ± 327.88	170.80 ± 7.27	−40.56	6.4	0.121 ± 0.0504	−52.97
<i>Icam1</i>	Intercellular adhesion molecule 1	9381.98 ± 327.39	4649.03 ± 116.46	−2.02	1	0.530 ± 0.0945	−1.89
<i>IL-1b</i>	Interleukin-1 α	584.02 ± 32.38	129.32 ± 5.08	−4.52	1.42	0.348 ± 0.0898	−4.08
<i>Irf1</i>	Interferon regulatory factor 1	3486.07 ± 165.70	1359.24 ± 35.10	−2.56	1.82	0.359 ± 0.1453	−5.07
<i>Itgal</i>	Integrin βL	340.80 ± 15.87	96.47 ± 3.43	−3.53	0.00209	0.000 ± 0.0001	−4.57
<i>Mapkapk2</i>	MAP kinase-activated protein kinase 2	7214.01 ± 503.98	2006.96 ± 51.12	−3.59	143.7	34.000 ± 18.6663	−4.23
<i>Myd116</i>	Myeloid differentiation primary response gene 116	266.25 ± 22.84	1620.09 ± 49.08	6.08	0.0239	0.293 ± 0.1803	0.08
<i>Nos2</i>	Nitric oxide synthase 2, inducible, macrophage	2027.58 ± 165.12	462.84 ± 12.12	−4.38	192.5	27.733 ± 9.3661	−6.94
<i>Tnfrsf1b</i>	Tumor necrosis factor receptor superfamily, member 1b	108.84 ± 7.44	86.05 ± 3.55	−1.26	0.131	0.015 ± 0.0093	−8.46
<i>Tyk2</i>	Tyrosine kinase 2	248.51 ± 17.67	123.86 ± 4.80	−2.01	0.00498	0.004 ± 0.0001	−1.41

Genes were selected for real-time RT-PCR analysis from the list of differentially expressed genes.

*Average hybridization signal (±SEM).

**Conc ratio (±Conc ratio STD).

The correlation coefficient between mRNA expression values determined by microarray hybridization and real-time RT-PCR was $R^2 = 0.88$.

Upon BHG treatment, IκB was up-regulated. As IκB and NFκB are part both of the glucocorticoid receptor and IL-10 signaling routes, it can be assumed that they might play an important role for mediating BHG's effects. This point of view is supported by a previous finding with phytochemical NO inhibitors [31–34] and synthetic compounds [49]. Since BHG both inhibited NO and up-regulated IκB in the present investigation, the role of NFκB and IκB for BHG's activity deserves further investigation.

Glucocorticoids exert their effects by binding to glucocorticoid receptor (GR). The immunomodulatory action of glucocorticoids is thought to be due to its inhibitory role on the activity of transcription factors, such as activator protein-1 (AP-1) and NFκB that are involved in the activation of pro-inflammatory genes. Consequently, glucocorticoids suppress the production and effects of humoral factors involved in inflammatory response and inhibit leukocytes' migration to the inflammation sites. It has been

suggested that glucocorticoid resistance in acute alopecia may be related to the disturbance of GR activity, which is partly due to the decreased thioredoxin reductase 1 (TXNRD1) activity and is affected by redox status of intracellular environment. In addition, dominant negative TXN significantly inhibited the TXNRD1 effect on GR raising the possibility that thioredoxin reductase 1 enhances GR activity through reduction of thioredoxin [50–53]. Interestingly, the initial computational screening of the present investigation revealed a significant correlation between *TXNRD1* mRNA expression and IC₅₀ values for BHG led to the identification as candidate NO inhibitor.

In the past, glucocorticoids were used for treatment of sepsis, and NO plays a central role in the pathophysiology of sepsis [54]. As glucocorticoids exert severe side effects with increased mortality rates, steroid treatment of sepsis was ceased [55]. Recently, NO inhalation for therapy of sepsis was discussed [56]. This indicates that NO might interfere with the glucocorticoid signaling pathway affecting sepsis. Our microarray data with BHG favor this hypothesis, since BHG both inhibited NO synthesis and regulated mRNA expression of genes involved in glucocorticoid signaling [57].

The fact that BHG affects the IL-10 signaling pathway in the present investigation also points to a possible mechanistic cross-talk. The effective control of airway inflammation exerted by glucocorticoids in asthma is largely mediated by inhibition of the transcriptional activity of several different genes encoding pro-inflammatory proteins such as cytokines, including IL-10, and mediator-synthesizing enzymes, including iNOS [58]. NO is generated by macrophages and macrophage-like cells commonly associated with cell-mediated immunity. NO production is stimulated by LPS, INF- γ and other activation signals and inhibited by a number of cytokines (especially interleukin-4, interleukin-10, and transforming growth factor- β) [59]. The interplay of IL-10, NO, and glucocorticoids may have consequences for the therapy of airway inflammatory diseases [60].

In conclusion, we identified BHG as an NO production inhibiting compound that interferes with the glucocorticoid receptor and IL-10 signaling pathways. The therapeutic potential of this compound has to be explored in the future.

Acknowledgment

This study was funded by the Dietmar Hopp-Foundation, Germany, by a grant to V.B.K.

Appendix A. Supplementary data

Supplementary data associated with this article can be found, in the online version, at doi:10.1016/j.bcp.2010.01.020.

References

- [1] Anggard E. Nitric oxide: mediator, murderer, and medicine. *Lancet* 1994;343:1199–206.
- [2] Lechner M, Lirk P, Rieder J. Inducible nitric oxide synthase (iNOS) in tumor biology: the two sides of the same coin. *Semin Cancer Biol* 2005;15:277–89.
- [3] Wink DA, Kasprzak KS, Maragos CM, Elespuru RK, Misra M, Dunams TM, et al. DNA deaminating ability and genotoxicity of nitric oxide and its progenitors. *Science* 1991;254:1001–3.
- [4] Schmutte C, Rideout 3rd WM, Shen JC, Jones PA. Mutagenicity of nitric oxide is not caused by deamination of cytosine or 5-methylcytosine in double stranded DNA. *Carcinogenesis* 1994;15:2899–903.
- [5] Felley-Bosco E. Role of nitric oxide in genotoxicity: implication for carcinogenesis. *Cancer Metastasis Rev* 1998;17:25–37.
- [6] Li CQ, Trudel LJ, Wogan GN. Nitric oxide-induced genotoxicity, mitochondrial damage, and apoptosis in human lymphoblastoid cells expressing wild-type and mutant p53. *Proc Natl Acad Sci USA* 2002;99:10364–9.
- [7] Sawa T, Ohshima H. Nitric oxide DNA damage in inflammation and its possible role in carcinogenesis. *Nitric Oxide* 2006;14:91–100.
- [8] Murakami A, Ohgashi H. Targeting NOX, iNOS and COX-2 in inflammatory cells: chemoprevention using food phytochemicals. *Int J Cancer* 2007;121:2357–63.
- [9] Perwez Hussain S, Harris CC. Inflammation and cancer: an ancient link with novel potentials. *Int J Cancer* 2007;121:2373–80.
- [10] Ridnour LA, Thomas DD, Donzelli S, Espey MG, Roberts DD, Wink DA, et al. The biphasic nature of nitric oxide responses in tumor biology. *Antioxid Redox Signal* 2006;8:1329–37.
- [11] Bentz BG, Haines 3rd GK, Lingen MW, Pelzer HJ, Hanson DG, Radosevich JA. Nitric oxide synthase type 3 is increased in squamous hyperplasia, dysplasia, and squamous cell carcinoma of the head and neck. *Ann Otol Rhinol Laryngol* 1999;108:781–7.
- [12] Tanaka H, Kijima H, Tokunaga T, Tajima T, Himeno S, Kenmochi T, et al. Frequent expression of inducible nitric oxide synthase in esophageal squamous cell carcinomas. *Int J Oncol* 1999;14:1069–73.
- [13] Jang TJ, Kim DK. Inducible nitric oxide synthase expression of tumor and stromal cells is associated with the progression of 7,12-dimethylbenz[a]anthracene-induced rat mammary tumors. *Cancer Lett* 2002;182:121–6.
- [14] Franco L, Doria D, Bertazzoni E, Benini A, Bassi C. Increased expression of inducible nitric oxide synthase and cyclooxygenase-2 in pancreatic cancer. *Prostaglandins Other Lipid Mediat* 2004;73:51–8.
- [15] Speranza L, De Lutiis MA, Shaik YB, Felaco M, Patruno A, Tetè A, et al. Localization and activity of iNOS in normal human lung tissue and lung cancer tissue. *Int J Biol Markers* 2007;22:226–31.
- [16] Chen HH, Su WC, Chou CY, Guo HR, Ho SY, Que J, et al. Increased expression of nitric oxide synthase and cyclooxygenase-2 is associated with poor survival in cervical cancer treated with radiotherapy. *Int J Radiat Oncol Biol Phys* 2005;63:1093–100.
- [17] Li LG, Xu HN. Inducible nitric oxide synthase, nitrotyrosine and apoptosis in gastric adenocarcinomas and their correlation with a poor survival. *World J Gastroenterol* 2005;11:2539–44.
- [18] Wang L, Shi GG, Yao JC, Gong W, Wei D, Wu TT, et al. Expression of endothelial nitric oxide synthase correlates with the angiogenic phenotype of and predicts poor prognosis in human gastric cancer. *Gastric Cancer* 2005;8:18–28.
- [19] Ekmekcioglu S, Ellerhorst JA, Prieto VG, Johnson MM, Broemeling LD, Grimm EA. Tumor iNOS predicts poor survival for stage III melanoma patients. *Int J Cancer* 2006;119:861–6.
- [20] Badn W, Hegardt P, Fellert MA, Darabi A, Esbjörnsson M, Smith KE, et al. Inhibition of inducible nitric oxide synthase enhances anti-tumour immune responses in rats immunized with IFN- γ -secreting glioma cells. *Scand J Immunol* 2007;65:289–97.
- [21] Frederiksen LJ, Sullivan R, Maxwell LR, Macdonald-Goodfellow SK, Adams MA, Bennett BM, et al. Chemosensitization of cancer in vitro and in vivo by nitric oxide signalling. *Clin Cancer Res* 2007;13:2199–206.
- [22] Hirst DG, Robson T. Nitrosative stress in cancer therapy. *Front Biosci* 2007;12:3406–18.
- [23] Calixto JB, Campos MM, Otuki MF, Santos AR. Anti-inflammatory compounds of plant origin. Part II. Modulation of pro-inflammatory cytokines, chemokines and adhesion molecules. *Planta Med* 2004;70:93–103.
- [24] Wang CC, Huang YJ, Chen LG, Lee LT, Yang LL. Inducible nitric oxide synthase inhibitors of Chinese herbs III. *Rheum palmatum*. *Planta Med* 2002;68:869–74.
- [25] Dirsch VM, Stuppner H, Vollmar AM. The Griess assay: suitable for a bio-guided fractionation of anti-inflammatory plant extracts? *Planta Med* 1998;64:423–6.
- [26] Park HJ, Kim RG, Seo BR, Ha J, Ahn BT, Bok SH, et al. Saucerin-7 and saucerin-8 isolated from *Saururus chinensis* inhibit the LPS-induced production of nitric oxide and prostaglandin E2 in macrophage RAW264.7 cells. *Planta Med* 2003;69:947–50.
- [27] Yun JM, Kwon H, Hwang JK. In vitro anti-inflammatory activity of panduratin A isolated from *Kaempferia pandurata* in RAW264.7 cells. *Planta Med* 2003;69:1102–8.
- [28] Jang SI, Jeong SI, Kim KJ, Kim HJ, Yu HH, Park R, et al. Tanshinone IIA from *Salvia miltiorrhiza* inhibits inducible nitric oxide synthase expression and production of TNF- α , IL-1 β and IL-6 in activated RAW 264.7 cells. *Planta Med* 2003;69:1057–9.
- [29] Jiang DJ, Jiang JL, Tan GS, Huang ZZ, Deng HW, Li YJ. Demethylbellidifolin inhibits adhesion of monocytes to endothelial cells via reduction of tumor necrosis factor alpha and endogenous nitric oxide synthase inhibitor level. *Planta Med* 2003;69:1150–2.
- [30] Radtke OA, Kiderlen AF, Kayser O, Kolodziej H. Gene expression profiles of inducible nitric oxide synthase and cytokines in *Leishmania major*-infected macrophage-like RAW 264.7 cells treated with gallic acid. *Planta Med* 2004;70:924–8.
- [31] Won JH, Kim JY, Yun KJ, Lee JH, Back NI, Chung HG, et al. Gigantol isolated from the whole plants of *Cymbidium goeringii* inhibits the LPS-induced iNOS and COX-2 expression via NF- κ B inactivation in RAW 264.7 macrophages cells. *Planta Med* 2006;72:1181–7.
- [32] Lin CM, Huang ST, Liang YC, Lin MS, Shih CM, Chang YC, et al. Isovitexin suppresses lipopolysaccharide-mediated inducible nitric oxide synthase through inhibition of NF- κ B in mouse macrophages. *Planta Med* 2005;71:748–53.
- [33] Ko HC, Kuo YH, Wei BL, Chiou WF. Laxifolone A suppresses LPS/IFN- γ -induced NO synthesis by attenuating NF- κ B translocation: role of NF- κ B p105 level. *Planta Med* 2005;71:514–9.
- [34] Jin XY, Lee SH, Kim JY, Zhao YZ, Park EJ, Lee BS, et al. Polyozellin inhibits nitric oxide production by down-regulating LPS-induced activity of NF- κ B and SAPK/JNK in RAW 264.7 cells. *Planta Med* 2006;72:857–9.

- [35] Park KM, Kim YS, Jeong TC, Joe CO, Shin HJ, Lee YH, et al. Nitric oxide is involved in the immunomodulating activities of acidic polysaccharide from *Panax ginseng*. *Planta Med* 2001;67:122–6.
- [36] Kolodziej H, Kayser O, Kiderlen AF, Ito H, Hatano T, Yoshida T, et al. Antileishmanial activity of hydrolyzable tannins and their modulatory effects on nitric oxide and tumour necrosis factor- α release in macrophages in vitro. *Planta Med* 2001;67:825–32.
- [37] Guerrero MF, Puebla P, Martín ML, Carrón R, San Román L, Reguero MT, et al. Inhibitory effect of N(G)-nitro-L-arginine methyl ester on the anti-adrenergic response elicited by ayanin in the pithed rat. *Planta Med* 2002;68:322–5.
- [38] Lahlou S, Magalhães PJ, Carneiro-Leão RF, Leal-Cardoso JH. Involvement of nitric oxide in the mediation of the hypotensive action of the essential oil of *Mentha × villosa* in normotensive conscious rats. *Planta Med* 2002;68:694–9.
- [39] Estrada S, Rojas A, Mathison Y, Israel A, Mata R. Nitric oxide/cGMP mediates the spasmolytic action of 3,4'-dihydroxy-5,5'-dimethoxybibenzyl from *Scaphyglottis livida*. *Planta Med* 1999;65:109–14.
- [40] Konkimalla VB, Efferth T. Anti-cancer natural product library from traditional chinese medicine. *Comb Chem High Throughput Screen* 2008;11:7–15.
- [41] Lee KH, Ibuka T, Sims D, Muraoka O, Kiyokawa H, Hall IH, et al. Antitumor agents. 44. Bis(helenaliny) esters and related derivatives as novel potent antileukemic agents. *J Med Chem* 1981;24:924–7.
- [42] Jorens PG, Matthys KE, Bult H. Modulation of nitric oxide synthase activity in macrophages. *Mediators Inflamm* 1995;4:75–89.
- [43] Kleinert H, Schwarz PM, Förstermann U. Regulation of the expression of inducible nitric oxide synthase. *Biol Chem* 2003;384:1343–64.
- [44] Konkimalla VB, Blunder M, Korn B, Soomro SA, Jansen H, Chang W, et al. Effect of artemisinins and other endoperoxides on nitric oxide-related signaling pathway in RAW 264.7 mouse macrophage cells. *Nitric Oxide* 2008;19:184–91.
- [45] Baer HP, Schmidt K, Mayer B, Kukovetz WR. Pentamidine does not interfere with nitrite formation in activated RAW 264.7 macrophages but inhibits constitutive brain nitric oxide synthase. *Life Sci* 1995;57:1973–80.
- [46] Wippel R, Rehn M, Gorren ACF, Schmidt K, Mayer B. Interference of the polyphenol epicatechin with the biological chemistry of nitric oxide- and peroxynitrite-mediated reactions. *Biochem Pharmacol* 2004;67:1285–95.
- [47] Scudiero DA, Shoemaker RH, Paull KD, Monks A, Tierney S, Nofziger TH, et al. Evaluation of a soluble tetrazolium/formazan assay for cell growth and drug sensitivity using human and other tumor cell lines. *Cancer Res* 1988;48:4827–33.
- [48] Eberwine J, Yeh H, Miyashiro K, Cao Y, Nair S, Finnel R. Analysis of gene expression in single live neurons. *Proc Natl Acad Sci USA* 1992;89:3010–4.
- [49] Huerta-Yepez S, Vega M, Jazirehi A, Garban H, Hongo F, Cheng G, et al. Nitric oxide sensitizes prostate carcinoma cell lines to TRAIL-mediated apoptosis via inactivation of NF- κ B and inhibition of Bcl-xL expression. *Oncogene* 2004;23:4993–5003.
- [50] Comtois SL, Gidley MD, Kelly DJ. Role of the thioredoxin system and the thiol-peroxidases Tpx and Bcp in mediating resistance to oxidative and nitrosative stress in *Helicobacter pylori*. *Microbiology* 2003;149(Pt 1):121–9.
- [51] Calabrese V, Sultana R, Scapagnini G, Guagliano E, Sapienza M, Bella R, et al. Nitrosative stress, cellular stress response, and thiol homeostasis in patients with Alzheimer's disease. *Antioxid Redox Signal* 2006;8:1975–86.
- [52] Sun Y, Rigas B. The thioredoxin system mediates redox-induced cell death in human colon cancer cells: implications for the mechanism of action of anticancer agents. *Cancer Res* 2008;68:8269–77.
- [53] Sohn KC, Jang S, Choi DK, Lee YS, Yoon TJ, Jeon EK, et al. Effect of thioredoxin reductase 1 on glucocorticoid receptor activity in human outer root sheath cells. *Biochem Biophys Res Commun* 2007;356:810–5.
- [54] Fernandes D, Duma D, Assreuy J. Steroids and nitric oxide in sepsis. *Front Biosci* 2008;13:1698–710.
- [55] Boyer A, Chadda K, Salah A, Annane D. Glucocorticoid treatment in patients with septic shock: effects on vasopressor use and mortality. *Int J Clin Pharmacol Ther* 2006;44:309–18.
- [56] Goldfarb RD, Cinel I. Inhaled nitric oxide therapy for sepsis: more than just lung. *Crit Care Med* 2007;35:290–2.
- [57] Suzuki H. New insight from the interplay between nitric oxide and glucocorticoids. *Crit Care Med* 2004;32:2362–3.
- [58] Stellato C. Post-transcriptional and nongenomic effects of glucocorticoids. *Proc Am Thorac Soc* 2004;1:255–63.
- [59] James SL. Role of nitric oxide in parasitic infections. *Microbiol Rev* 1995;59:533–47.
- [60] Ogawa Y, Duru EA, Ameredes BT. Role of IL-10 in the resolution of airway inflammation. *Curr Mol Med* 2008;8:437–45.